# Synthesis, Characterization, and Thermal Degradation Kinetic of Polystyrene-*g*-Polycaprolactone

**Yeliz Yildirim, Buket Doğan, Sinem Muğlali, Fehmi Saltan, Melek Özkan, Hakan Akat***

*Department of Chemistry, Faculty of Science, Ege University, Bornova, Izmir 35100, Turkey*

Received 28 July 2011; accepted 27 January 2012
DOI 10.1002/app.36888
Published online in Wiley Online Library (wileyonlinelibrary.com).

**ABSTRACT:** In the present study, it has been demonstrated that polystyrene-*g*-polycaprolactone (PS-*g*-PCL) was successfully prepared by "click chemistry." For this purpose, first, poly(styrene-*co*-4-chloromethylstyrene) (P(S-*co*-CMS)) with 4-chloromethylstyrene content (10%) was synthesized. Second, alkyne-functionalized polycaprolactone (PCL) was obtained using propargyl alcohol and caprolactone. P(S-*co*-CMS) and PCL were reacted in *N*,*N*-dimethylformamide for 24 h at 25°C to give PS-*g*-PCL. The synthesized polymer was characterized by nuclear magnetic resonance ($^1$H-NMR), gel permeation chromatography, Fourier transform infrared spectroscopy and thermogravimetric analysis. The apparent activation energies for thermal degradation of PS-*g*-PCL were obtained by differential (Kissenger) and integral methods (Flynn–Wall–Ozawa, Kissinger–Akahira–Sunose, Tang, Coats–Redfern, Van Krevelen et al.). The decomposition mechanism and pre-exponential factor were calculated in terms of Coats–Redfern method. The most likely decomposition processes of first and second degradation stages were $A_n$ type and $F_3$ type, respectively.
 J Appl Polym Sci 000: 000–000, 2012

**Key words:** thermal degradation; polymer synthesis; click chemistry; polyesters

## INTRODUCTION

In last 5 years, polystyrene (PS) and polycaprolactone (PCL) have managed to become one of the world's most widely used polymers. PS is one of the three standard plastics (polyolefins, poly(vinyl chloride), and PS), and PS can be applied in many fields, such as the packaging of electrical equipment, apparatus, instruments, and foods, thermal insulation materials for buildings and cold storage, and disposable dinner service. Unfortunately, PS does not degrade naturally, and this leads to millions of tons for white pollution, that is, waste foam PS, annually. The recycling or utilization of polymer waste saves raw materials and protects the environment to which much attention has been directed recently.[1]

PCL is synthetic polyester obtained by the self-condensation of the cyclic ester epsilon-caprolactone.[2] PCL has unique properties that make it attractive for biomaterials applications. Like most synthetic polymers, it has excellent water-resistant properties. At the same time, like most natural polymers, it has excellent biodegradability and biocompatibility properties. These properties have made it possible for PCL to be used in a variety of biomaterial applications including drug release,[3] medical devices,[4] cell cultivation/cell culture,[5] and biodegradable packaging materials.[6–8] In recent years, there are many studies about PS and PCL polymers. Generally, the studies are about block or blends of polymers.[9,10] As PS is widely used polymer, we have synthesized PS-$N_3$ to prepare a polystyrene-*g*-polycaprolactone (PS-*g*-PCL) via click chemistry method which is widely used these days. The "click"-type reactions, mainly hold up as by Huisgen 1,3-dipolar azide-alkyne[11–14], [3 + 2], or have attracted much attention owing to their important features including high yields, high tolerance of functional groups, and selectivity.[15] Huisgen 1,3-dipolar cycloaddition occurs between an alkyne and an organic azide to give triazole ring. The reactions can be performed under mild experimental conditions when catalyzed by copper (I). The development and the application of click chemistry in polymer and material science has been recently studied extensively.

The study of degradation of PS-*g*-PCL is important in understanding their usability for processing, application, and thermal recycling. The common methods of polymer degradation are biodegradation, photo-oxidative degradation, ozone-induced degradation, mechanochemical degradation, thermal degradation, and catalytic degradation.[16–19] The degradation of grafted polymer of PS and PCL has not been studied. Therefore, the influence of PCL on the thermal stability of PS was also investigated.

*Correspondence to:* H. Akat (hakan.akat@ege.edu.tr).

## KINETIC METHODS

Thermogravimetric analysis (TGA) can be used for the determination of degradation kinetic a lot of polymer.[20–22] In general, the thermal degradation reaction of a solid polymer can be shown as:

$$A_{\text{solid}} \rightarrow B_{\text{solid}} + C_{\text{gas}}$$

where $A$ is the starting material, $B_{\text{solid}}$ and $C_{\text{gas}}$ are the solid residue and the gas product, respectively.

The kinetic of thermal degradation of polymers is generally expressed by the following typical kinetic equation

$$r = d\alpha/dt = k(T) \times f(\alpha) \quad (1)$$

where $T$ is the absolute temperature (in K), $r$ is the rate of change conversion or composition per unit time ($t$) and $f(\alpha)$ is the conversion function (reaction model). The conversion degree ($\alpha$) was calculated with eq. (2), where $m_o$, $m_t$, and $m_f$ are the weights of sample before degradation, at time $t$, and after complete degradation, respectively.

$$\alpha = m_o - m_t/m_o - m_f \quad (2)$$

where $k$ is the reaction constant which can be expressed by the Arrhenius equation:

$$k(T) = Ae^{-(Ea/RT)} \quad (3)$$

where $A$ is the pre-exponential factor, $E_a$ is activation energy, and $R$ is the gas constant.

By combining eqs. (1) and (3), the following equation is obtained

$$d\alpha/dt = Ae^{-(Ea/RT)}f(\alpha) \quad (4)$$

According to nonisothermal kinetic theory, the fractional conversion $\alpha$ is expressed as a function of temperature, which is dependent on the time of heating. Thus, the heating rate ($\beta$) can be described as:

$$\beta = dT/dt \quad (5)$$

Equation (4) is modified as follows:

$$d\alpha/dT = (1/\beta)Ae^{-(Ea/RT)}f(\alpha) \quad (6)$$

Equations (4) and (6) are the basis for the many equations derived to evaluate thermal analysis data.

A number of methods for the calculation of kinetic parameters $A$, $E$, $n$ based on integral or differential methods are used.

## DIFFERENTIAL METHOD

### Kissinger method

Activation energy can be calculated using eq. (7) with Kissinger method without knowing the solid-state degradation reaction mechanism.[23,24]

$$\ln(\beta/T^2_{\max}) = \ln AR/E_a + \ln(n[1-\alpha_{\max}]^{n-1}) - (E/RT_{\max}) \quad (7)$$

where $\beta$ is heating rate, $T_{\max}$ is temperature related to maximum reaction rate, $A$ is pre-exponential factor, $\alpha_{\max}$ is maximum degradation fraction, $n$ is reaction order. Plotting $\ln(\beta/T^2_{\max})$ versus $(1000/T_{\max})$ gives activation energy from slope.

## INTEGRAL METHODS

### Flynn–Wall–Ozawa method

This method is one of the integral methods that can be used to determine the activation energy without knowledge of reaction mechanism.[21,25] Pre-exponential factor ($A$) and activation energy ($E_a$) do not depend on degradation fraction, but they depend on the temperature. This method uses eq. (8).

$$\log g(\alpha) = \log(AE_a/R) - \log\beta + \log\ p(E/RT) \quad (8)$$

Doyle approximation is used and eq. (8) can be obtained.

$$\log\beta = \log(AE_a/R) - \log\ g(\alpha) - 2.315 - 0.4567(E/RT) \quad (9)$$

The plot of log $\beta$ versus 1000/T should be linear with the slope $E_a/R$ from which $E_a$ can be obtained.

### Kissinger–Akahira–Sunose method

The activation energy can be determined by Kissinger–Akahira–Sunose (KAS) method,[22,24] using the following equation

$$\ln(\beta/T2) = \ln AR/E_a g(\alpha - (E_a/RT) \quad (10)$$

According to this method, the plots of $\ln(\beta/T^2)$ versus $1000/T$ at same $\alpha$-value give straight lines with slope equals to $-E_a/R$.

### Tang method

The Tang method[26,27] is based on the following equation:

$$\ln(\beta/T^{1.894661}) = \ln\ AE_a/Rg(\alpha) + 3.635041 - 1.894661 \ln\ E_a - (1.001450E_a/RT) \quad (11)$$

the plot of $\ln(\beta/T^{1.894661})$ versus $1000/T$ can give $E_a$ from slope.

**TABLE I**
**Algebraic Expressions of $f(\alpha)$ and $g(\alpha)$ for the Reaction Models Considered in the Present study[25–27]**

| Symbol | Reaction model | $f(\alpha)$ | $g(\alpha)$ |
|---|---|---|---|
| **Sigmoidal curves** | | | |
| $A_2$ | Avrami–Erofeey ($n = 2$) (nucleation and growth) | $2(1-\alpha)[-\ln(1-\alpha)]^{1/2}$ | $[-\ln(1-\alpha)]^{1/2}$ |
| $A_3$ | Avrami–Erofeey ($n = 3$) (nucleation and growth) | $3(1-\alpha)[-\ln(1-\alpha)]^{2/3}$ | $[-\ln(1-\alpha)]^{1/3}$ |
| $A_4$ | Avrami–Erofeey ($n = 4$) (nucleation and growth) | $4(1-\alpha)[-\ln(1-\alpha)]^{3/4}$ | $[-\ln(1-\alpha)]^{1/4}$ |
| $A_n$ | Avrami–Erofeey ($n = n$) (nucleation and growth) | $n(1-\alpha)[-\ln(1-\alpha)]^{(n-1)/n}$ | $[-\ln(1-\alpha)]^{1/n}$ |
| **Acceleration curves** | | | |
| $P_1$ | Power law | $4\alpha^{3/4}$ | $\alpha^{1/4}$ |
| $P_2$ | Power law | $3\alpha^{2/3}$ | $\alpha^{1/3}$ |
| $P_3$ | Power law | $2\alpha^{1/2}$ | $\alpha^{1/2}$ |
| $P_4$ | Power law | $2/3\alpha^{-1/2}$ | $\alpha^{3/2}$ |
| **Deceleration curves** | | | |
| $R_1$ | Zero-order (Polany–Winger equation) Phase boundary-controlled reaction (one-dimensional movement) | 1 | $\alpha$ |
| $R_2$ | Phase boundary-controlled reaction (contracting area, that is, bidimensional shape) | $2(1-\alpha)^{1/2}$ | $[1-(1-\alpha)^{1/2}]$ |
| $R_3$ | Phase boundary-controlled reaction (contracting area, that is, bidimensional shape) | $3(1-\alpha)^{2/3}$ | $[1-(1-\alpha)^{1/3}]$ |
| $F_1$ | First order (Mampel) (random nucleation with two nucleus on the individual particle) | $(1-\alpha)$ | $-\ln(1-\alpha)$ |
| $F_2$ | Second order (random nucleation with two nucleus on the individual particle) | $(1-\alpha)^2$ | $(1-\alpha)^{-1}-1$ |
| $F_3$ | Third order (random nucleation with two nucleus on the individual particle) | $(1-\alpha)^3$ | $(1/2)[(1-\alpha)^{-2}-1]$ |
| $D_1$ | One-dimensional diffusion | $1/2\alpha$ | $A^2$ |
| $D_2$ | Two-dimensional diffusion (bidimensional particle shape) Valensi equation | $1/[-\ln(1-\alpha)]$ | $(1-\alpha)\ln(1-\alpha)+\alpha$ |
| $D_3$ | Three-dimensional diffusion (tridimensional particle shape) Jander equation | $3(1-\alpha)^{1/3}/2[(1-\alpha)^{-1/3}-1]$ | $[1-(1-\alpha)^{1/3}]^2$ |
| $D_4$ | Three-dimensional diffusion (tridimensional particle shape) Ginstling–Brounshtein | $3/2[(1-\alpha)^{-1/3}-1]$ | $(1-2\alpha/3)-(1-\alpha)^{2/3}$ |

### Coats–Redfern method

This method[28,29] is based on eq. (12)

$$\ln(g(\alpha)/T^2) = \ln(AR/E_a\beta - (E_a/RT) \qquad (12)$$

A straight line can be obtained from the line which is drawn between ln $(g(\alpha)/T^2)$ versus $1000/T$. The slope of the line gives $-E/R$. The possible thermal degradation mechanism can also be obtained. The most commonly used reaction models for solid-state processes are listed in Table I.

### Van Krevelen et al. method

Van krevelen et al. method[30,31] is found to be the first theoretical expression from TG data. They use an approximation for exponential integral to obtain eq. (13).

$$\log g(\alpha) = \log B + (E_a/RT_r + 1)\ \log\ T \qquad (13)$$

where

$$B = A/\beta(E_a/RT_r - 1)^{-1}(0.386/T_r)^{E/RT_r} \qquad (11)$$

$T_r$ is a reference temperature. The slope of line drawn between log $g(\alpha)$ versus log $T$ gives activation energy.

## EXPERIMENTAL

### Materials

Styrene (S, 99%, Sigma-Aldrich Company, USA) and 4-chloromethylstyrene (CMS, ca. 60/40 meta/para isomer mixture, 97%, Sigma-Aldrich Company, USA) were distilled under reduced pressure before use. 2,2′-Azobis(isobutyronitrile) (AIBN, 98%, Sigma-Aldrich Company, USA) was recrystallized from ethanol. *N*-oxyl-free radical (TEMPO, 99%, Sigma-Aldrich Company, USA) was used as received. Tetrahydrofuran (THF, 99.8%, J.T. Baker Company, Holland) was dried and distilled over benzophenone-Na. Other solvents were purified by conventional procedures. Triethylamine (98%, Sigma-Aldrich Company, USA) and dichloromethane (99.9%, HPLC grade, Sigma-Aldrich Company, USA) were distilled from $CaH_2$. Ethylenediaminetetraacetic acid (EDTA + 99%, Sigma-Aldrich Company, USA) *N*,*N*-dimethylformamide (DMF + 99%, Sigma-Aldrich Company, USA). Epsilon-caprolactone (CL + 99%, Sigma-Aldrich Company, USA).

Propargyl alcohol (99%, Sigma-Aldrich Company, USA) were used without any purification.

### Instrumentation

$^1$H NMR (NMR, nuclear magnetic resonance) measurements were recorded in $CDCl_3$ (deuterium chloroform) with $Si(CH_3)_4$ as internal standard, using Varian AS-400 (400 MHz) instrument. Fourier transform infrared spectroscopy (FTIR) spectra were recorded on a PerkinElmer FTIR Spectrum One-B spectrometer. UV spectra were recorded on a Shimadzu UV-1601 spectrometer. Molecular weights were determined by gel permeation chromatography (GPC) instrument equipped with a Waters styragel column (HR series 2, 3, 5E) with THF as the eluent at a flow rate of 0.3 mL/min and a Waters 410 differential refractometer detector.

TG measurements of powders polymer samples were obtained on PerkinElmer Diamond TA/TGA from 25 to 600°C at different heating rates (5, 10, 15, and 20°C/min), under constant flow rate of 100 mL/min of nitrogen atmosphere. The sample weights for all the experiments were taken in the range of 8–10 mg.

### Synthesis of poly(styrene-*co*-chloromethylstyrene)

Poly(styrene-*co*-4-chloromethylstyrene) (P(S-*co*-CMS)) with 4-chloromethylstyrene content (10%) was synthesized as described previously.[14]

### Synthesis of polystyrene-azide (PS-$N_3$)

A typical procedure for the preparation of PS-$N_3$ from 10 mol % CMS containing P(S-*co*-CMS) is as follows: P(S-*co*-CMS) (1.0 g, $1.04 \times 10^{-4}$ mol) was dissolved in DMF, and $NaN_3$ (0.07 g, $1.01 \times 10^{-3}$ mol) was added. The resulting solution was allowed to stir at 25°C overnight and precipitated in excess methanol/water mixture (1/1 by volume). $^1$H NMR ($CDCl_3$): δ ppm) 7.40–6.20 (b, 9H), 4.25 (s, 2H) FTIR %$T$ ($cm^{-1}$): 3060, 2924, 2096, 1681, 1601, 1492, 1453, 757, 698. $M_n$: 3500 g/mol PDI: 1.50.

### Synthesis of alkyne-functionalized PCL

Alkyne-functionalized poly(epsilon-caprolactone) (PCL) was obtained according to the methods described previously in the literature[7] by ROP of CL using $Sn(Oct)_2$ as a catalyst and propargyl alcohol as an initiator. Typically, propargyl alcohol (0.019 mol) and CL (0.13 mol) were charged in a 50-mL Schlenk flask with a magnetic stirring bar, and a solution of $Sn(Oct)_2$ ($20.10^{-4}$ mol) in 0.5 mL of toluene was also added using a syringe. The reactive mixture was degassed via three pump-freeze–thaw cycles and then immersed in a thermostatic oil bath at 110°C for 7 h.

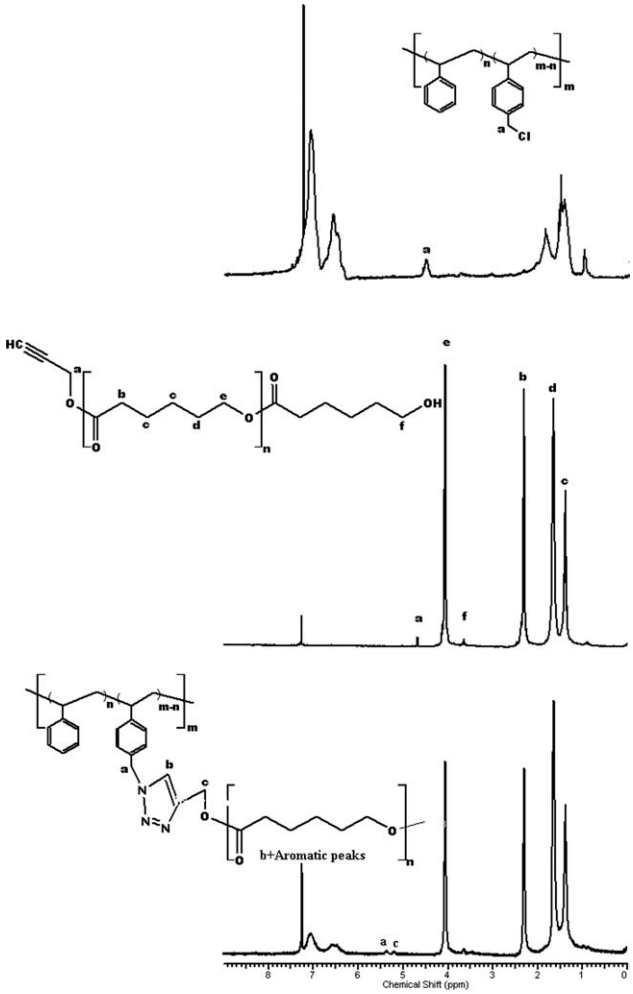


**Figure 1** $^1$HNMR spectra of PS-$N_3$, PCL, and PS-*g*-PCL.

The obtained solid was dissolved in THF, and the solution was dropped into an excessive amount of methanol. The product was dried under vacuum overnight with a yield of 80%.$^1$H NMR ($CDCl_3$), d (TMS, ppm): 4.66 (s, 2H, $CH_2$—C≡CH), 4.00 (m, $CH_2O$ on PCL), 3.65 (t, 2H, $CH_2OH$), 2.50 (s, 1H, $CH_2$—C≡CH), 2.35–2.27 (m, $CH_2$-C=O), 1.67–1.57 (m, $CH_2$), 1.40–1.38 (m, $CH_2$).GPC: $M_n = 7500$ g/mol, PDI = 1.29. Calculated $M_{n(\text{calc})} = 6700$ g/mol.

### Preparation of the PS-*g*-PCL by "click" chemistry

In a flask, above obtained PS-$N_3$ (0.1 g, $1.04 \times 10^{-5}$ mol) and alkyne-functionalized PCL (0.335 g, $6.21 \times 10^{-5}$ mol), copper (I) bromide (0.192 g, $9.0 \times 10^{-5}$ mol), 2,2′-Bipyridine (0.017 g, $1.09 \times 10^{-4}$ mol), and dry DMF (5 mL) were added. The flask was capped with a septum and purged with dry nitrogen for 10 min. The mixture was stirred overnight at ambient temperature. After removing the catalyst by EDTA, functionalized polymer was precipitated in methanol (200 mL), filtered, and dried under vacuum. $^1$H

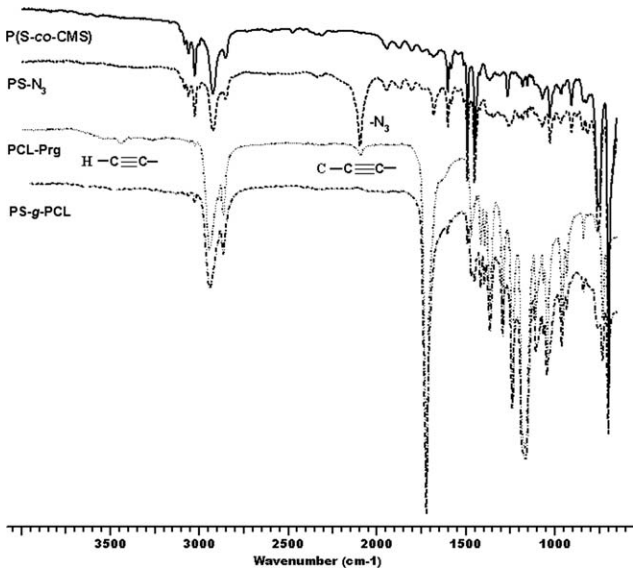


**Figure 2** FTIR spectra of P(S-*co*-CMS), PS-$N_3$, PCL-Prg, and PS-*g*-PCL.

NMR, FTIR spectra, and GPC chromatogram of the polymers are shown in Figures 1–3, respectively.

$$M_n = 13,500 \text{ g/mol, PDI : } 1.90.$$

## RESULTS AND DISCUSSION

As stated in the introduction section, our synthetic approach toward the direct preparation of grafted polymer is based on "click" chemistry strategy. The overall process is shown in Scheme 1. According to this approach, first P(S-*co*-CMS), copolymer containing two different 4-chloromethylstyrene (CMS) units (10%) were prepared via nitroxide-mediated radical polymerization. The compositions of copolymers as determined by using $^1$H NMR spectroscopy are in agreement with the expected values and indicate the

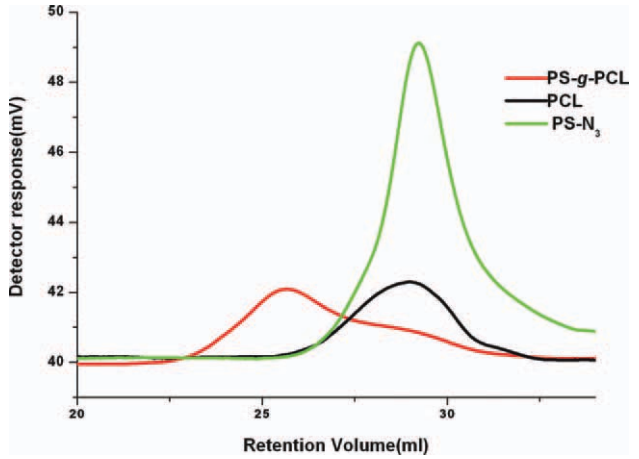


**Figure 3** GPC traces of PS-$N_3$, PCL-Prg, and PS-*g*-PCL. [Color figure can be viewed in the online issue, which is available at wileyonlinelibrary.com.]

random copolymer structure. The resulting P(S-*co*-CMS) copolymer was then quantitatively converted into polystyrene-azide (PS-$N_3$) in the presence of $NaN_3$/DMF at room temperature. Figure 1 shows $^1$H NMR spectrum of polymer. Although the signal at 4.25 ppm corresponding to —$CH_2$—$N_3$ protons of the precursor, PS-$N_3$ shifted to new signal appeared at 5.35 ppm was attributed to —$CH_2$ linked to triazole ring. The FTIR spectral analysis also supports this result (Fig. 2). The other components of the click reaction, namely alkyne-functionalized poly(epsilon-caprolactone), were synthesized according to the literature procedure.[7]

Alkyne-functionalized PCL precursor was prepared by ROP of CL in bulk using $Sn(Oct)_2$ as a catalyst and propargyl alcohol as an initiator and the molar ratio of [CL] : [propargyl alcohol] : [$Sn(Oct)_2$] = 4000 : 100 : 1. The $^1$H NMR spectrum of alkyne-PCL showed the resonance signals of protons —$CH_2$—C≡CH at 4.66 and 2.50 ppm, and protons of repeating unit of PCL at 2.35–2.27, 1.67–1.57, 1.40–1.38, and 4.00 ppm, whereas the signals of protons —$CH_2$—OH at 3.65 ppm were still observed, which indicated that ROP has completed. We have also calculated $M_n$ according to $^1$H NMR results. When we compare the two results, we can see the alignment between them. In the final step of the process, PS-$N_3$ and PCL were reacted in one-pot to yield the desired PS-*g*-PCL polymer.

TG curves and the corresponding derivative curves (DTG) for PS-*g*-PCL are shown in Figure 4. The derivative of the thermogram with respect to temperature, also known as a differential thermogram or DTG, indeed shows the maximum rate of polymer decomposition ($T_{max}$). The degradation of the polymer shows two main stages. The first-stage reaction appears to begin around 220°C and stop around 350°C with maximum rate at 337°C for heating rate 5°C/min. The second-stage reaction appears between 350 and 440°C with maximum rate of weight loss around 409°C for heating rate 5°C/min. The TG characteristics initial temperature of a decomposition process ($T_i$), maximum degradation temperature ($T_{max}$), final temperature of a decomposition process ($T_f$), and residual mass ($1 - \alpha$) are listed in Table II at the different heating rates (5, 10, 15, and 20°C/min). As the heating rate increased, degradation onset temperatures of the DTG curves and maximum degradation temperatures increased. While a small amount of ash contents remained for PS-*g*-PCL above 600°C after this temperature, there was no observable char residue for PS and PCL.[18,32] The residue for PS-*g*-PCL may be owing to some secondary reactions in high temperatures. As shown in Figure 4 and Table I, the quantities of ash that remain after thermal degradation of the PS-*g*-PCL sample with increasing heating rates have values

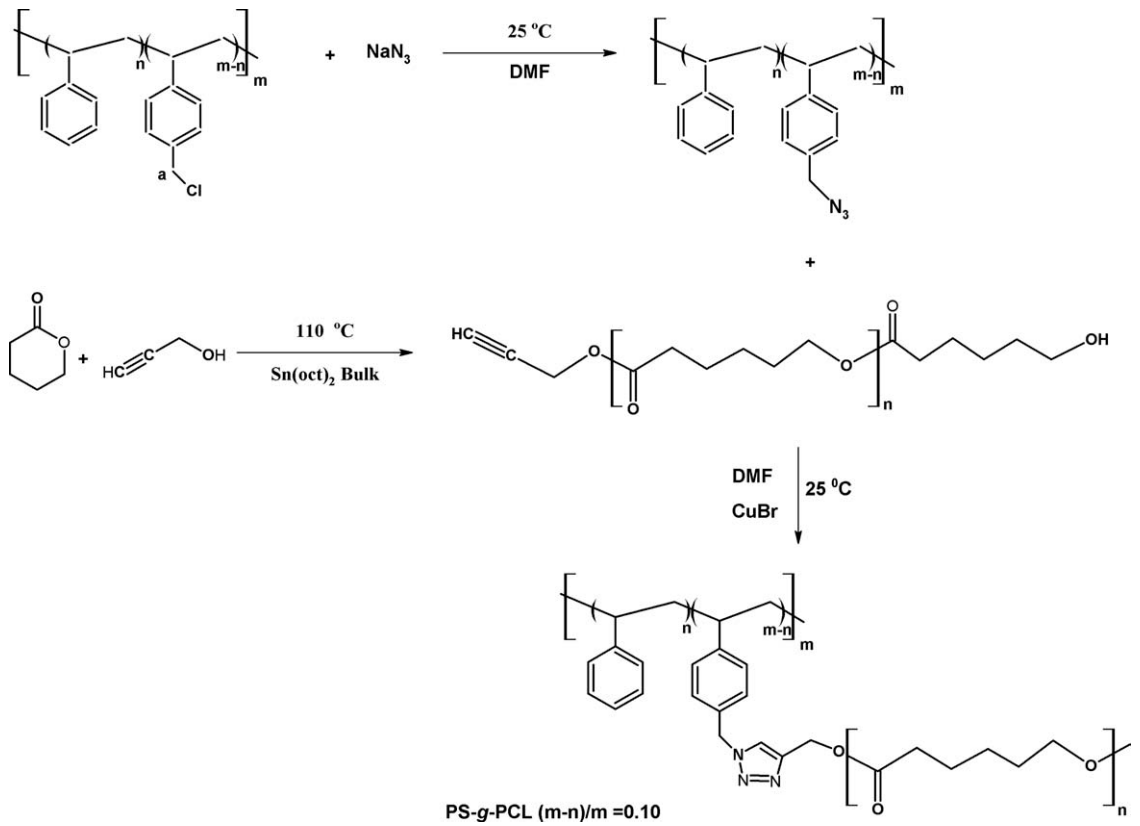


**Scheme 1** Synthesis of PS-*g*-PCL via click chemistry.

between 29.89 and 31.15 for first and 13.77–14.12 for second decomposition stage.

Another result is that the polymer decomposes 70% for first stage and 16% for second stage. As mentioned above, grafted ratio of PS-*g*-PCL is 10% PCL units onto PS. Compared to decomposition of fraction, we can say that mostly first stage of the PS-*g*-PCL is related to PS and second stage of that is about to PCL.

Consequently, the first ($T_{max1}$) maximum decomposition was in the range of 337–364°C and it was owing to the destruction of PS part of the polymer. The analysis of thermodestruction of PS and PCL was described earlier.[18,32–34] PS has been reported to degrade by two steps. In the first step, it is assumed that random scissions break the polymer chains at weak points, resulting from factors such as head-to-head linkages, chain branches, and unsaturated bonds. In the second step, the shorter chain segments depolymerize into volatile products consisting mainly of monomer and low-molecular-weight oligomers (e.g., dimer, trimer, and tetramers).[32] The various products obtained from the pyrolysis of PS are styrene (major product 40 and 60%), toluene (1–2%), and α-methylstyrene (0.5%).[33] Reaction schemes of formation of these products were published for PS by McNeill et al.[33] The second maximum of decomposition ($T_{max2}$) was in the range of 409–433°C and was owing to the degradation of PCL. The thermal degradation of PCL has been reported to degrade in a two-stage degradation mechanism (both random chain scission and specific chain end scission).[34] That is, the first step (nearly 380°C) is a random rupture of the polyester chains via cis-elimination reaction which produces $H_2O$, $CO_2$, and 5-hexanoic acid, and the second step (up to 400°C) is an unzipping depolymerization process at the chain-ends with hydroxyl end groups to form CL.[16,35] At lower temperatures, random chain scission dominates the degradation and as the temperature increases the specific chain end scission (from the hydroxyl chain end of the chain) dominates, suggesting the change in dominating mechanism during the degradation under dynamic heating. Reaction schemes of the formation of the CL were published for PCL by Aoyagi et al.[17] The decomposition of PS/PCL blends was studied by Mohamed et al. and showed one, two, or three decomposition stage depending on the blend composition. Although the blend with 75 : 25 PCL : PS showed only one transition, the higher PS content (50 : 50 PCL : PS and 25 : 75 PCL : PS) in blends showed two and three transitions, respectively.[10]

At the same time, $T_{max}$, $T_i$, and $T_f$ for PS-*g*-PCL are lower than that for PS and PCL in all heating rates. A similar behavior to PCL/PS blend was

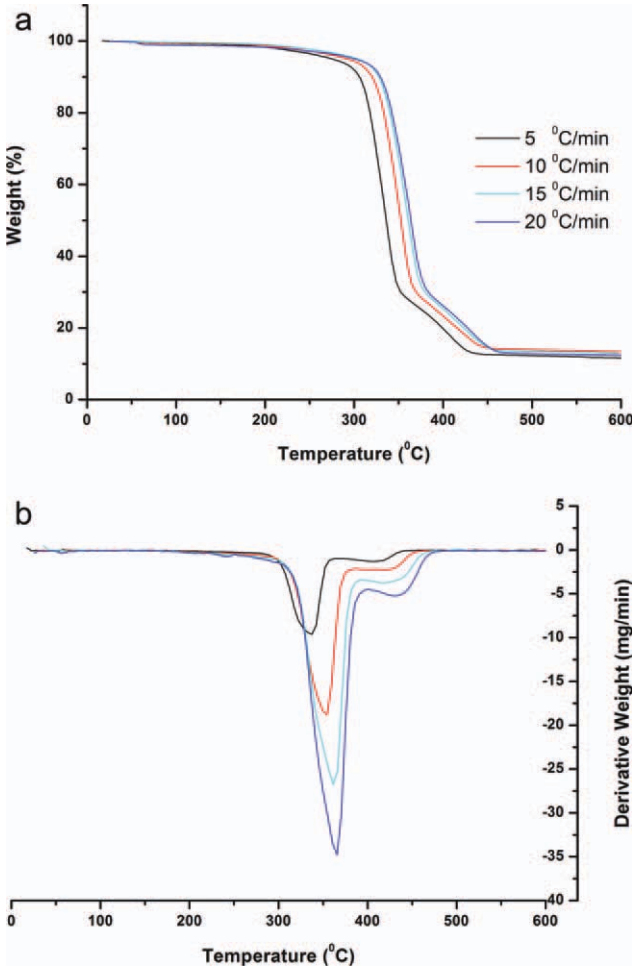


**Figure 4** (a) Typical TG and (b) DTG curves for the PS-*g*-PCL sample in $N_2$ atmosphere at different heating rates (5, 10, 15, and 20°C/min). [Color figure can be viewed in the online issue, which is available at wileyonlinelibrary.com.]

obtained by Mohamed et al. Clearly, PS and PCL are thermally more stable than PS-*g*-PCL, because the thermal decomposition of PS and PCL initiates at higher temperatures compared to PS-*g*-PCL. This may be ascribed to the incorporation of PCL onto PS that interferes with the degradation mechanisms of PCL and PS and affects the degradation pathway of PS-*g*-PCL. This phenomenon occurs owing to the special unknown mechanism in this random-grafted polymer degradation process.

To obtain more information about thermal stability of the PS-*g*-PCL, kinetic parameters (activation energy and pre-exponential factor) were calculated using differential and integral methods. The kinetic studies were also carried out to investigate the degradation mechanisms for two degradation stages.

The Kissinger, Flynn–Wall–Ozawa, TANG, and KAS methods were first employed to analyze the TG data of PS-*g*-PCL because they were independent of any thermal degradation mechanism.

The activation energies and correlations obtained from the classical method of Kissinger for PS-*g*-PCL are 151 ± 7 kJ/mol ($r^2$ = 0.9950) for the first stage and 207 ± 9 kJ/mol ($r^2$ = 0.9789) for the second stage.

Plotting log β and $1000/T$ as a function of conversation according to the Flynn–Wall–Ozawa method is shown in Figure 5. The mean value activation energies obtained by Tang method were calculated from the slope of the ln ($\beta/T^{1.894661}$) versus $1000/T$ as 155 ± 15 kJ/mol (for first stage) and 179 ± 31 kJ/mol (for second stage). Finally, KAS method is based on eq. (10) and requires several thermograms (at least four) at different heating rates. The values of activation energies were determined from plots of $\ln(\beta/T^2)$ versus $1000/T$ at same α-value. Table III summarizes the activation energies of first and second stages obtained by the Flynn–Wall–Ozawa, TANG, and KAS methods.

The values in case of the calculated activation energies of PS-*g*-PCL are compared; the values obtained from Kissinger method were higher than those from Flynn–Wall–Ozawa, KAS, Tang, Coats–Redfern, Van Krevelen et al. especially in the second stage. It may be owing to the fact that second peaks on DTG curves were not sharp enough to determine the peak point and this broadness might bring some difference.

The $E_a$ as a function of % conversion is commonly used as indicator for the degradation mechanism, that is, one-step or more degradation mechanism. The variation of activation energy versus conversion of PS-*g*-PCL is an evidence of the complex degradation mechanism (probably parallel or consecutive reactions[17,36]) This behavior was observed in the range of $0.05 \leq \alpha \leq 0.40$ and $0.40 \leq \alpha \leq 0.60$ for first

**TABLE II**
**Initial Temperature of a Decomposition Process ($T_i$), Maximum Degradation Temperature ($T_{max}$), Final Temperature of a Decomposition Process ($T_f$), and Residual Mass (α)**

| Heating Rate (β) (°C/min) | $T_i$ (°C) | | $T_{max}$ (°C) | | $T_f$ (°C) | | Residue (1 − α) at 600°C | |
|---|---|---|---|---|---|---|---|---|
| | First stage | Second stage | First stage | Second stage | First stage | Second stage | First stage | Second stage |
| 5 | 200.0 | 347.7 | 337.0 | 409.0 | 347.7 | 431.2 | 29.89 | 13.77 |
| 10 | 200.6 | 364.3 | 351.0 | 423.0 | 364.3 | 449.8 | 30.07 | 13.93 |
| 15 | 201.6 | 375.0 | 360.0 | 431.0 | 375.0 | 450.4 | 30.59 | 14.01 |
| 20 | 202.6 | 381.8 | 364.0 | 433.0 | 381.8 | 462.8 | 31.15 | 14.12 |

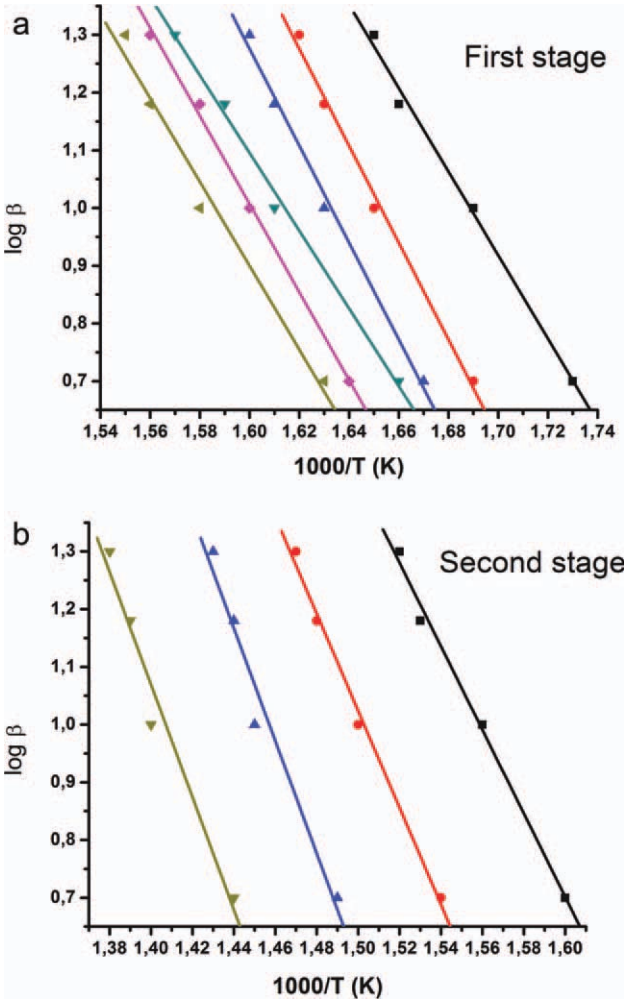


**Figure 5** The logarithm of heating rate versus temperature at constant conversion (a) for first stage (0.10, 0.20, 0.30, 0.40, 0.50, and 0.60) and (b) second stage (0.70, 0.75, 0.80, and 0.85) for the degradation of PS-*g*-PCL. [Color figure can be viewed in the online issue, which is available at wileyonlinelibrary.com.]

stage and hence distinctly in the range of $0.70 \leq \alpha \leq 0.75$ and $0.80 \leq \alpha \leq 0.85$ for second stage.

The activation energies of PS were calculated as between 154 and 260 kJ/mol as a function of molecular weight.[32] The activation energies of PCL for specific chain scission stage (second stage) were calculated as 180 ± 7 kJ/mol,[36] 149 ± 9 kJ/mol,[37], 179 ± 7 kJ/mol,[37] 232 ± 7 kJ/mol,[16] and 201 kJ/mol[18] by using different kinetic methods. The average activation energies obtained using Kissinger, Flynn–Wall–Ozawa, KAS, and Tang methods were calculated 151 ± 7, 143 ± 12, 146 ± 18, 155 ± 15 kJ/mol for first stage, and 207 ± 9, 160 ± 35, 171 ± 30, 179 ± 31, 162 ± 3, 179 ± 9 kJ/mol for second stage, respectively. When the calculated activation energies of grafted polymer compared with pure PS and PCL, thermal stability of PS-*g*-PCL was found to be lower in comparison to those of given in the literature, especially for first stage.

The Coats–Redfern method was employed to investigate the thermal degradation mechanism of PS-*g*-PCL by comparing the activation energies obtained from the above four methods. Table IV summarizes the activation energies and correlations obtained from the slope of the $\ln(g(\alpha)/T^2)$ versus $1000/T$ at different heating rates. Analysis of the Table IV shows that at all the heating rate values, the activation energies are in better agreement with that of obtained using Flynn–Wall–Ozawa method $A_n$ type for first stage at a heating rate 15°C/min. For the second stage, comparing the activation energies in Table III with three methods, the values obtained by Flynn–Wall–Ozawa, 160 ± 35 kJ/mol, were very close to 162 ± 5 kJ/mol from $F_3$ type at a heating rate 20°C/min.

To confirm the degradation reaction mechanism of PS-*g*-PCL, we have calculated activation energies and correlations using Van Krevelen et al. method.

**TABLE III**
**The Degradation Activation Energies of PS-*g*-PCL Calculated by Flynn–Wall–Ozawa, TANG, and KAS Methods**

| | Flynn–Wall–Ozawa | | TANG | | KAS | |
|---|---|---|---|---|---|---|
| | | | First stage | | | |
| α | *E* (kJ/mol) | $r^2$ | *E* (kJ/mol) | $r^2$ | *E* (kJ/mol) | $r^2$ |
| | | | First stage | | | |
| **0.1** | 131.7 | 0.9925 | 147.6 | 0.9934 | 150.8 | 0.9913 |
| **0.2** | 152.9 | 0.9923 | 170.1 | 0.9931 | 150.8 | 0.9913 |
| **0.3** | 152.9 | 0.9923 | 170.2 | 0.9931 | 150.7 | 0.9776 |
| **0.4** | 152.9 | 0.9949 | 148.6 | 0.9829 | 150.4 | 0.9913 |
| **0.5** | 138.9 | 0.9978 | 148.1 | 0.9931 | 150.5 | 0.9776 |
| **0.6** | 132.2 | 0.9806 | 148.7 | 0.9829 | 128.6 | 0.9913 |
| **Mean** | 143 ± 12 | | 155 ± 15 | | 146 ± 18 | |
| | | | Second stage | | | |
| α | *E* (kJ/mol) | $r^2$ | *E* (kJ/mol) | $r^2$ | *E* (kJ/mol) | $r^2$ |
| **0.7** | 131.7 | 0.9925 | 148.4 | 0.9935 | 157.5 | 0.9912 |
| **0.75** | 152.9 | 0.9923 | 171.0 | 0.9932 | 149.8 | 0.9914 |
| **0.80** | 177.8 | 0.9676 | 199.2 | 0.9983 | 177.3 | 0.9860 |
| **0.85** | 177.8 | 0.9676 | 197.8 | 0.9931 | 200.8 | 0.9913 |
| **Mean** | 160 ± 35 | | 179 ± 31 | | 171 ± 30 | |

**TABLE IV**
**The Degradation Activation Energies of PS-*g*-PCL Calculated by Using Coats–Redfern Method at Different Heating Rates (5, 10, 15, and 20°C/min)**

| β (°C/min) | 5 | | | | 10 | | | | 15 | | | | 20 | | | |
|---|---|---|---|---|---|---|---|---|---|---|---|---|---|---|---|---|
| Symbol | First stage *E* (kJ/mol) | $r^2$ | Second stage *E* (kJ/mol) | $r^2$ | First stage *E* (kJ/mol) | $r^2$ | Second stage *E* (kJ/mol) | $r^2$ | First stage *E* (kJ/mol) | $r^2$ | Second stage *E* (kJ/mol) | $r^2$ | First stage *E* (kJ/mol) | $r^2$ | Second stage *E* (kJ/mol) | $r^2$ |
| $A_2$ | 125.9 | 0.9260 | 25.42 | 0.9820 | 129.7 | 0.9490 | 24.83 | 0.9820 | **141.9** | 0.9710 | 31.82 | 0.9930 | 126.8 | 0.9650 | 35.37 | 0.9810 |
| $A_3$ | 125.9 | 0.9260 | 25.42 | 0.9820 | 129.7 | 0.9490 | 24.83 | 0.9820 | **141.9** | 0.9710 | 31.82 | 0.9930 | 126.8 | 0.9650 | 35.37 | 0.9810 |
| $A_4$ | 125.9 | 0.9260 | 25.42 | 0.9820 | 129.7 | 0.9490 | 24.83 | 0.9820 | **141.9** | 0.9710 | 31.82 | 0.9930 | 126.8 | 0.9650 | 35.37 | 0.9810 |
| $R_1$ | 106.8 | 0.9430 | 1.610 | 0.9520 | 109.8 | 0.9640 | 2.200 | 0.9730 | 119.5 | 0.9750 | 1.150 | 0.9320 | 106.8 | 0.9710 | 2.120 | 0.9240 |
| $R_2$ | 23.28 | 0.9400 | 13.06 | 0.9990 | 21.92 | 0.9400 | 13.65 | 0.9990 | 22.12 | 0.9810 | 12.63 | 0.9970 | 20.69 | 0.9660 | 11.99 | 0.9990 |
| $R_3$ | 9.130 | 0.8660 | 16.25 | 0.9990 | 8.200 | 0.8500 | 16.84 | 0.9990 | 8.310 | 0.9460 | 16.29 | 0.9990 | 7.890 | 0.9030 | 15.91 | 0.9990 |
| $D_1$ | 223.2 | 0.9480 | 18.67 | 0.9980 | 229.5 | 0.9670 | 18.08 | 0.9980 | 249.2 | 0.9770 | 23.89 | 0.9880 | 223.6 | 0.9740 | 27.09 | 0.9970 |
| $D_2$ | 235.0 | 0.9430 | 31.55 | 0.9970 | 241.7 | 0.9630 | 30.96 | 0.9970 | 262.9 | 0.9770 | 38.77 | 0.9950 | 235.9 | 0.9730 | 42.94 | 0.9950 |
| $D_3$ | 28.21 | 0.9380 | 10.60 | 0.9990 | 26.60 | 0.9350 | 11.19 | 0.9990 | 27.00 | 0.9780 | 9.790 | 0.9940 | 13.80 | 0.8890 | 8.960 | 0.9970 |
| $D_4$ | 19.10 | 0.8540 | 39.29 | 0.9970 | 27.57 | 0.9260 | 39.88 | 0.9970 | 29.00 | 0.9800 | 42.89 | 0.9980 | 27.69 | 0.9780 | 44.27 | 0.9960 |
| $F_1$ | 125.9 | 0.9260 | 24.83 | 0.9820 | 129.7 | 0.9490 | 24.83 | 0.9820 | 141.9 | 0.9710 | 31.82 | 0.9930 | 126.8 | 0.9650 | 35.37 | 0.9810 |
| $F_2$ | 148.4 | 0.9020 | 70.18 | 0.9800 | 152.9 | 0.9260 | 69.59 | 0.9780 | 168.2 | 0.9590 | 83.66 | 0.9900 | 150.3 | 0.9510 | 90.42 | 0.9760 |
| $F_3$ | 173.9 | 0.8760 | 129.2 | 0.9760 | 179.5 | 0.9010 | 128.6 | 0.9800 | 198.2 | 0.9420 | 152.0 | 0.9870 | 177.1 | 0.9590 | **162.9** | 0.9780 |
| $P_1$ | 19.42 | 0.9010 | 16.82 | 0.9990 | 19.96 | 0.9380 | 17.41 | 0.9990 | 22.25 | 0.9570 | 16.96 | 0.9880 | 19.04 | 0.9470 | 16.62 | 0.9990 |
| $P_2$ | 29.12 | 0.9200 | 15.13 | 0.9990 | 29.94 | 0.9490 | 15.72 | 0.9990 | 33.05 | 0.9650 | 15.01 | 0.9980 | 28.79 | 0.9680 | 14.54 | 0.9990 |
| $P_3$ | 48.53 | 0.9330 | 11.75 | 0.9990 | 49.90 | 0.9580 | 12.34 | 0.9990 | 54.67 | 0.9710 | 11.12 | 0.9940 | 48.27 | 0.9660 | 10.37 | 0.9990 |
| $P_4$ | 165.0 | 0.9460 | 8.530 | 0.9960 | 169.6 | 0.9660 | 7.940 | 0.9950 | 184.3 | 0.9760 | 12.22 | 0.9730 | 165.2 | 0.9730 | 14.60 | 0.9950 |

**TABLE V**
**Activation energies Obtained Using Van Krevelen et al. Method for Sigmoidal $A_n$ Mechanism (First Decomposition Stage) and Decelerated $F_3$ Mechanism (Second Decomposition Stage) at Different Heating Rates (5, 10, 15, and 20°C/min)**

| β (°C/min) | 5 | | 10 | | 15 | | 20 | |
|---|---|---|---|---|---|---|---|---|
| Symbol | First stage $E$ (kJ/mol) | $r^2$ | First stage $E$ (kJ/mol) | $r^2$ | First stage $E$ (kJ/mol) | $r^2$ | First stage $E$ (kJ/mol) | $r^2$ |
| $A_2$ | 137.4 | 0.9433 | 140.6 | 0.9622 | 152.3 | 0.9786 | 137.5 | 0.9747 |
| $A_3$ | 137.4 | 0.9433 | 140.6 | 0.9622 | 152.3 | 0.9786 | 137.5 | 0.9747 |
| $A_4$ | 137.4 | 0.9433 | 140.6 | 0.9622 | 152.3 | 0.9786 | 137.5 | 0.9747 |
| β (°C/min) | 5 | | 10 | | 15 | | 20 | |
| Symbol | Second stage $E$ (kJ/mol) | $r^2$ | Second stage $E$ (kJ/mol) | $r^2$ | Second stage $E$ (kJ/mol) | $r^2$ | Second stage $E$ (kJ/mol) | $r^2$ |
| $F_1$ | 37.74 | 0.9961 | 37.18 | 0.9622 | 44.40 | 0.9981 | 48.12 | 0.9944 |
| $F_2$ | 84.22 | 0.9900 | 83.38 | 0.9901 | 97.74 | 0.9953 | 104.8 | 0.9874 |
| $F_3$ | 145.5 | 0.9861 | 144.3 | 0.9862 | 168.1 | 0.9930 | 179.5 | 0.9830 |

The activation energies and correlations value for $A_n$ and $F_3$ type at different heating rates are listed in Table V. As it can be seen, mechanism $A_n$, heating rates 20, 10, and 20°C/min, give the results in better agreement with that of obtained using Flynn–Wall–Ozawa, TANG, and KAS, respectively. Comparing the activation energies in Tables III and V for second degradation stage (mechanism $F_3$), heating rates 15, 20, and 15°C/min, the results were in best agreement with Flynn–Wall–Ozawa, TANG, and KAS methods, respectively.

Consequently, the solid-state decomposition mechanism for the first degradation stage of PS-*g*-PCL was a Sigmoidal curve $A_n$ type, nucleation, and growth mechanism and its rate-controlling process obeyed the Avrami–Erofeey equation with integral form $[-\ln(1-\alpha)]^{1/n}$. However, at the second degradation stage of PS-*g*-PCL, its solid-state decomposition mechanism corresponded to decelerated $F_3$ type, random nucleation with two nucleus on the individual particle with integral form $(1/2)[(1-\alpha)^{-2}-1]$.

### Determination of pre-exponential factor

The values of $A$ can be obtained by Coats–Redfern methods. The $A$ values of $A_2$, $A_3$, $A_4$, and $F_3$ are listed in Table VI.

**TABLE VI**
**Pre-Exponential Factor Obtained Using Coats–Redfern Method for Sigmoidal $A_n$ Mechanisms (First Decomposition Stage) at 15°C/min heating rates and Decelerated $F_3$ Mechanism (Second Decomposition Stage) at 20°C/min h2eating rates**

| Stage | Symbol | Pre-exponential factor $A$ ($min^{-1}$) |
|---|---|---|
| First stage | $A_2$ | $9.92 \times 10^{10}$ |
| | $A_3$ | $6.58 \times 10^{10}$ |
| | $A_4$ | $4.97 \times 10^{10}$ |
| | Mean ($A_n$) | $7.09 \times 10^{10}$ |
| Second stage | $F_3$ | $4.02 \times 10^{8}$ |

In the Coats–Redfern methods, $\ln A$ can be calculated from the intersection with the $y$ axis (when $x = 0$ and $y = \ln AR/\beta E_a$), knowing this equation:

$$\ln(g(\alpha)/T^2 = \ln(AR/E_a) - (E_a/RT) \qquad (13)$$

The pre-exponential factors obtained from eq. (13) are summarized in Table VI for the first and second stages.

## CONCLUSIONS

A new grafted polymer, PS-*g*-PCL, was synthesized with click chemistry method and it was characterized by FTIR, $^1$H-NMR, and TG–DTA techniques. The thermal degradation of PS-*g*-PCL in nitrogen is two-stage reaction. The thermal degradation kinetic of PS-*g*-PCL was evaluated by using six methods. The average activation energies for first stage obtained using Kissinger, Flynn–Wall–Ozawa, KAS, Tang, Coats–Redfern, and Van Krevelen et al. methods were calculated as 151 ± 7, 143 ± 12, 146 ± 18, 155 ± 15, 141 ± 3, and 141 ± 5 kJ/mol, respectively. The degradation mechanism and the average pre-exponential factor were determined by Coats–Redfern methods as $A_n$ type and $7.09 \times 10^{10}$, respectively. For the second stage, the average activation energy values from Kissinger, Flynn–Wall–Ozawa, KAS, Tang, Coats–Redfern, and Van Krevelen et al. methods were taken as 207 ± 9, 160 ± 35, 171 ± 30, 179 ± 31, 162 ± 3, 179 ± 9 kJ/mol, respectively. The degradation mechanism and the pre-exponential factor were determined by Coats–Redfern method as $F_3$ type and $4.02 \times 10^8$, respectively. Consequently; thermal stability of PS-*g*-PCL is found to be lower in comparison to those of pure PS and PCL.

## References


1. Ai, Z. Q.; Zhou, Q. L.; Guang, R.; Zhang, H. T. J Appl Polym Sci 2005, 96, 1405.
2. Smith, D. F.; Peacock, G. S.; Mead, B.; Salgado, O. M. Union City, 4751112, 1988.
3. Bei, J.; Wang, W.; Wang, Z.; Wang, S. Polym Adv Technol 1966, 7, 104.
4. Yasin, M.; Tighe, B. Biomaterials 1992, 13, 9.
5. Rouxhet, L.; Duhoux, F.; Borecky, O.; Legras, R.; Schneider, Y. J. J Biomater Sci Polym Ed 1998, 9, 1279.
6. Koenig, M. F.; Huang, S. J. Polymer 1995, 36, 1877.
7. Tasdelen, M. A. Eur Polym J 2011, 47, 937.
8. Biresaw, G.; Carriere, C. J. J Appl Polym Sci 2002, 83, 3145.
9. Shi, G. Y.; Yang, L. P.; Pan, C. Y. J Polym Sci A: Polym Chem 2008, 46, 6496.
10. Mohamed, A.; Gordon, S. H.; Biresaw, G. Polym Degrad Stab 2007, 92, 1177.
11. Huisgen, R. In 1,3-Dipolar Cycloaddition Chemistry; Padwa, A., Ed.; Wiley: New York, 1984; pp 1-176.
12. Rostovtsev, V. V.; Green, G.; Fokin, V. V.; Sharpless, K. B. Angew Chem Int Ed 2002, 41, 2596.
13. Akat, H.; Ozkan, M.; Expr Polym Lett 2011, 5, 318.
14. Gacal, B.; Akat, H.; Balta, D. K.; Arsu, N.; Yagci, Y. Macromolecules 2008, 41, 2401.
15. Lutz, J.-F. Angew Chem Int Ed 2007, 46, 1018.
16. Sivalingam, G.; Madras, G. Polym Degrad Stab 2004, 84, 393.
17. Aoyagi, Y.; Yamashita, K.; Doi, Y. Polym Degrad Stab 2002, 76, 53.
18. Sivalingam, G.; Madras, G. Polym Degrad Stab 2003, 80, 11.
19. Singh, B.; Sharma, N. Polym Degrad Stab 2008, 93, 561.
20. Lee, S.; Jin, B. S.; Lee, J. W. Macromol Res 2006, 14, 491.
21. Wang, D.; Das, A.; Leuteritz, A.; Boldt, R.; Häußler, L.; Wagenknecht, U.; Heinrich, G. Polym Degrad Stab 2011, 96, 285.
22. Yuzay, I. E.; Auras, R.; Soto-Valdez, Selke, H. S. Polym Degrad Stab 2010, 95, 1769.
23. Badia, J. D.; Santonja-Blasco, L.; Morina, R.; Ribes-Greus, A. Polym Degrad Stab 2010, 95, 2192.
24. Hamciuc, C.; Vlad-Bubulac, T.; Petreus, O.; Lisa, G. Eur Polym J 2007, 43, 980.
25. Fraga, F.; Nũñez, E. R. J Appl Polym Sci 2001, 80, 776.
26. Dogan, F.; Akat, H.; Balcan, M.; Kaya, I.; Yurekli, M. J Appl Polym Sci 2008, 108, 2328.
27. Janković, B.; Adnađević, B.; Jovanović, J. Thermochim Acta 2007, 452, 106.
28. Ou, C. Y.; Zhang, C. H.; Li, S. D.; Yang, L.; Dong, J. J.; Mo, X. L.; Zeng, M. T. Carbohydr Polym 2010, 82, 1284.
29. Sun, J. T.; Huang, Y. D.; Gong, G. F.; Cao, H. L. Polym Degrad Stab 2006, 91, 339.
30. Chang, T. C.; Wu, K. H.; Chiu, Y. S. Polym Degrad Stab 1999, 63, 103.
31. Nũñez, L.; Fraga, F.; Nũñez, M. R.; Villanueva, M. Polymer 2000, 41, 4635.
32. Malhotra, S. L.; Hesse J.; Blanchard, L. P. Polymer 1975, 16, 81.
33. McNeill, I. C.; Zulfigar, M.; Kousar, T. Polym Degrad Stab 1990, 28, 131.
34. Sivalingam, G.; Karthik, R.; Madras, G. J Anal Appl Pyrol 2003, 70, 631.
35. Persenaire, O.; Alexandre, M.; Degee, P.; Dubois, P. Biomacromolecules 2001, 2, 288.
36. Kim, K. J.; Doi, Y.; Abe, H.; Martin, D. P. Polym Degrad Stab 2006, 91, 2333.
37. Joshi, P.; Madras, G. Polym Degrad Stab 2008, 93, 1901.